Evaluating the Atibaia River Hydrology using JULES6.1

Hsi-Kai Chou[1], Ana Maria Heuminski de Avila [2], Michaela Bray[1]

[1]School of Engineering, Cardiff University, Cardiff, CF24 3AA, UK

[2]Center for Meteorological and Climate Research Applied to Agriculture (CEPAGRI) at the State University of Campinas, Campinas, SP 13083-871, Brazil

Correspondence to: Hsi-Kai Chou (ChouH2@cardiff.ac.uk)

Abstract.

Land surface models such as the Joint UK Land Environment Simulator (JULES) are increasingly used for hydrological assessments because of their state-of-the-art representation of physical processes and versatility. Unlike statistical models and AI models, the JULES model simulates the physical water flux under given meteorological conditions, allowing us to understand and investigate the cause and effect of environmental changes. Here we explore the possibility of this approach using a case study in the Atibaia river basin, which serves as a major water supply for metropolitan regions of Campinas and São Paulo, Brazil. The watershed is suffering increasing hydrological risks, which could be attributed to environmental changes, such as urbanization and agricultural activity. The increasing risks highlight the importance of evaluating the land surface processes of the watershed systematically. We explore the use of local precipitation collection complement with multiple sources of global reanalysis data to simulate the basin hydrology. Our results show that the coarse resolution of rainfall data is the main reason for reduced model performance. Despite this shortcoming, key hydrological fluxes in the basin can be represented by the JULES model simulations.

1 Introduction

The Atibaia river basin serves as a major water supply for Campinas and São Paulo (Demanboro et al., 2013; Nobre et al., 2016). The basin is subjected to human impacts such as urbanization and agricultural activities. Increasing hydrological risks have emerged with historic floods in 2009 and 2010 (de Campos & Celso Dal Ré, 2015), and drought in 2014 and 2015 (Marengo et al., 2015; Nobre et al., 2016), which highlight the importance of evaluating the hydrology systematically. Hydrological models are an essential tool in hydrological science and catchment management for evaluating the hydrological impacts of climate change or land-use and land-cover change (Buytaert & Beven, 2011). Up-to-date, a few research activities have investigated the Atibaia river basin due to its importance in the water supply (dos Santos et al., 2020; Prochmann, 2019).

Physically-based hydrological models are often used to simulate the physical water flux under given meteorological conditions, allowing us to understand and investigate the cause and effect of environmental changes. In which, a commonly used Soil Water Assessment Tool (SWAT) has been operated for flow and sediment estimation for the Atibaia river basin (dos

30   Santos et al., 2020). However, the accuracy of the model highly depends on the model structure, availability and quality of input data. Also, local calibration is usually required due to the few empirical approximations in each model.

    The JULES model was developed from the Met Office Surface Exchange Scheme (MOSES) by the UK Met Office (Cox et al., 1999). It can be coupled to an atmospheric global circulation model but is also used as a standalone land surface model which simulates the fluxes of carbon (Clark, D. B. et al., 2011), water, energy and momentum (Best et al., 2011) between the

35   land surface and the atmosphere. The model is driven by a large dataset of meteorological variables using a physically-based approach, and has been increasingly used for hydrological assessment (Le Vine et al., 2016; Martínez-de la Torre et al., 2019; Zulkafli et al., 2013). Therefore, we examine the model ability to simulate the land surface processes of the Atibaia watershed.

2 Methods and data

2.1 Study Region and da

40   This study explores the hydrology of the Atibaia River Basin. The altitude of the catchment ranges between 530 m and 1818 m; it is located between the coordinates 22°40′ and 23°30′ S and 47°30′ and 46°00′ W in south-eastern Brazil, covering an area of 2816.4 km^2 (Figure 1). For each sub-basin (17 sub-basins covering 128.8 km^2 in average, Figure 1), the surface ($Q_{surface}$) and sub-surface ($Q_{subsurface}$) runoff fluxes are simulated in gridbox with rainfall data from the nearest monitoring station (Campinas, Atibaia, and Nazare Paulista) of Campinas Agronomic Institute (Campinas-IAC). The year with high missing

45   rainfall records (e.g. 2012 and 2015) is replaced by using the time series from the nearest Department of Water and Electricity (DAEE) station of each grid. The modelling results cover 2075.2 km^2 effectively since Cachoeira Dam and Atibainha Dam intercept the upstream flow, and the monitor station does not cover part of the lower basin. The release data of the dams is used as the upstream flow, which is obtained from the Basic Sanitation Company of the State of Sao Paulo (SABESP, 2020). River flow observations from 3 stations (4D-009, 3D-006, 3E-063) measured by DAEE are used for model calibration and

50   validation.

    The primary soil types in this area are Ferralsols, Acrisols, Leptosols, and Cambisols (FAO/IIASA/ISRIC/ISSCAS/JRC, 2012; Ottoni et al., 2018; Rossi, 2017). The required soil parameters are obtained by using pedotransfer functions (PTFs) of Hodnett & Tomasella (2002), which generates parameters from physical and chemical properties of soil obtained from a large-scale soil database at 0.083 degree resolution (FAO/IIASA/ISRIC/ISSCAS/JRC, 2012).

55   The primary land cover is rural (53.0%), followed by forest (27.6%), and then urban (12.0%). Higher percentages of forest are found in the upper basin, whereas urban areas concentrate in the lower basin. We classified the land cover into five vegetated Plant Functional Types (Harper et al., 2018): including tropical broadleaf evergreen trees (BET-Tr), needle-leaf evergreen trees (NET), C3 grasses (C3), C4 grasses (C4), evergreen shrubs (ESH), and two non-vegetated: bare soil (BS) and urban (U) using MODIS data (Friedl & Sulla-Menashe, 2015) reclassified by Houldcroft et al. (2009).

60   The study region's rainfall presents a seasonal pattern with rainy summer and dry winter (Cavalcanti et al., 2017; Dias et al., 2013). The rainfall regimes are influenced by the passage and frontal systems' intensity (Maddox, 1983; Silveira et al.,

2016). The maximum precipitation occurs during the austral summer associated with the South Atlantic Convergence Zone (SACZ) and in the winter predominates the high pressing system of the South Atlantic (Jones & Carvalho, 2013). For this study, rainfall time series of from 2009 to 2019 are provided by 3 stations from Campinas-IAC and 5 stations from DAEE (Figure 1). The temperature, specific humidity, and surface pressure are observed by the Center for Meteorological and Climate Research Applied to Agriculture (CEPAGRI). The air temperature is elevation adjusted with the lapse rate (γ) 1.4 °C per 100 meters (Figure 2) obtained from Campinas-IAC and CEPAGRI data during the study period.

Other meteorological data required include downward short-wave radiation, long-wave radiation, and wind speed, all of which are extracted from the NCEP-DOE Reanalysis II dataset (Kanamitsu et al., 2002). The dataset is available on a T62 Gaussian grid with 192 x 94 points (approximately 2° scale) and provides a 6-hourly temporal resolution from 1979/01 up to the present. The 6-hourly resolution was disaggregated into hourly data using linear interpolation.

2.2 The JULES model

JULES simulates the energy exchange between different land surface processes described by Best et al. (2011) and Clark et al. (2011). For each sub-basin, distinct parameters are used to calculate the energy balance of surface temperatures, short-wave and long-wave radiative fluxes, sensible and latent heat fluxes, ground heat fluxes, canopy moisture contents, snow masses and snow melting rates for each surface type in a grid-box. The sub-grid surface heterogeneity is described using a tiled model upon a shared 4-layer soil column with a thickness of 0.1, 0.25, 0.65, and 2.0 m from top to bottom. In JULES, precipitation is intercepted by the canopy storage, then throughfall is then partitioned into surface flow and infiltration into the soil based on the Hortonian infiltration excess mechanism. JULES incorporates one of two different hydrologic models; 1) Probability Distributed Model (PDM) described by Moore (1985) and 2) TOPMODEL described by Beven and Kirkby, (1979). In our model setup, we have calculated saturation excess flow by first using the PDM , with the sub-grid distribution of soil moisture (θ) described by a probability function (Clark, Douglas B. & Gedney, 2008). The saturated fraction (f_{sat}) is described as:

$$f_{sat} = 1 - \left[1 - \frac{\max(0, S - S_0)}{S_{max} - S_0}\right]^{\frac{B}{B+1}} \tag{1}$$

S is the areal fraction of grid-box soil water storage. S_0 is the Minimum soil water content below which there is no surface runoff saturation excess production by PDM. S_{max} is the maximum grid-box storage, which equals to the volumetric soil water content (θ_s) multiple by the soil depth (Z_{pdm}). The shape parameter (B) is modified to better represent the subsurface flow (Clark, Douglas B. & Gedney, 2008). The parameter is initially set as 1, whereas values of 0.1/0.5 can be used for a more subsurface flow dominated hydrology, and a value of 10 for a more flash hydrological response. For the TOPMODEL approach the saturated fraction (f_{sat}) is found by integrating the pdf of the topographic index (λ). Numerical integration using a two-parameter gamma distribution can be found in Gedney and Cox (2003). Mean value and standard deviation of the topographic index data is obtained from Marthews et al. (2015) as follows:

$$f_{sat} = a_s \exp(-c_s f \lambda_{ic}) \tag{2}$$

in which, a_s and c_s are fitted parameters for each gridbox, λ_{ic} is the critical value of the topographic index at which the

95 water table reaches the surface, f is a decay parameter describing the decrease of the saturated hydraulic conductivity.

For both PDM and TOPMODEL, precipitation over the saturated fraction of the grid generates surface runoff. An instantaneous redistribution of soil moisture is assumed for the infiltration following the Darcy–Richards diffusion equation. The gravity drainage generates the subsurface flow at the lower boundaries.

We evaluated the sensitivity of hydrological parameters (Table 1) and calibrated the model to select the most suitable

100 approach for the study region. Soil hydraulic characteristics can be estimated using the relationship of Brooks & Corey (1964) or a more robust formulation of Van Genuchten (1980).

2.3 Model evaluation

The runoff fluxes simulated by the JULES model require an external river routing model for a reasonable comparison to observed river flows (Best et al., 2011). In this study, we applied a simple delayed function to account for the routing delay in

105 the river discharge (Q_{sim}) in each timestep (t). For each basin, the delay time (t_i) is dividing the distance to the outlet by flow speed (C). We set the flow speed constantly as the average flow speed of 0.36 m/s (from 2009 to 2019).

$$Q_{sim,t} = \sum_{i=1}^{n} \left(Q_{surface,t-t_{i1}} + Q_{subsurface,t-t_{i2}} \right); t_{i1} = \frac{d_i}{C_{surface}}; t_{i2} = \frac{d_i}{C_{subsurface}} \tag{3}$$

We evaluated the sensitivity of hydrological parameters of PDM and TOPMODEL to determine the most suitable model in the outlet of Atibaia river basin (4D-009) using the simulated results from the first year (2009). Soil depth (dz_pdm), shape

110 factor (b_pdm), the fraction of maximum storage (s_pdm) is evaluated for PDM, and a decay parameter describing the decrease of the saturated hydraulic conductivity (f) for the TOPMODEL. For PDM/TOPMODEL, the model is run from 2009 to 2019 with the parameter combination/value using the highest Nash Sutcliffe Efficiency (NSE) performance.

$$NSE = 1 - \frac{\sum_t^N \left(Q_{mod,t} - Q_{obs,t} \right)^2}{\sum_t^N \left(Q_{obs,t} - Q_{obs,mean} \right)^2} \tag{4}$$

Using the flow observed in the upper (3E-063), middle (3D-006), and lower basin (4D-009), we evaluated the overall

115 model performance using the NSE, RMSE-observations standard deviation ratio (RSR) , and percent bias (P_{BIAS}), following Moriasi et al. (2007):

$$RSR = \frac{\sqrt{\sum_t^N \left(Q_{obs,t} - Q_{mod,t} \right)^2}}{\sqrt{\sum_t^N \left(Q_{obs,t} - Q_{obs,mean} \right)^2}} \tag{5}$$

$$P_{BAIS} = \left(\frac{\sum_t^N Q_{obs,t} - \sum_t^N Q_{mod,t}}{\sum_t^N Q_{obs,t}} \right) * 100 \tag{6}$$

3 Results and Discussion

3.1 Sensitivity analysis

We evaluated the sensitivity of hydrological parameters in 1) the PDM and 2) TOPMODEL. For the PDM, we found lower flow simulated with increasing soil depth (Figure 3a). However, the average flow only reduced by 2.5 percent when soil depth was increased from 0.8 to 2.0. In contrast, we found that the shape factor (Figure 3b) and minimum soil water content (Figure 3c) have a higher impact on the simulated flow.

When we increased the minimum soil water content, the simulated flow is reduced with more water to be held on the soil. The average flow is reduced by 17.5 percent when the minimum soil water content increased from 0 to 4. We found gradual changes in the flow regime when adjusting the shape factor and minimum soil water content, whereas a higher value of the shape factor can change the flow into a subsurface flow-dominated regime (Figure 4a). We found that the shape factor of 0.5 best describes the flow in the study basin (NSE=0.49), as the higher shape factor simulates a more gradual flow regime (Clark, Douglas B. & Gedney, 2008), which in turn lowers the peak level flow estimation and hence increases baseflow generation (Figure 3b). We examined the model performance with a combination of soil depth, shape factor, and minimum soil water content, and found that the highest performance with combination dz=1.0, b=0.5, s=0, which altered the shape factor alone. Therefore, we run the full-time series of modelling with this parameter combination.

For TOPMODEL, we found that lower decay parameter increases the modelled flow (Figure 3d), especially in baseflow level (Figure 4b). In terms of model performance, we found a value of 3.0 simulates the highest NSE (0.61). The value is then selected to be used for the full model simulation.

3.2 Hydrological modelling using the JULES model

Table 2 summarize the evaluation of the JULES model in the upper, middle, and lower Atibaia river basin. We can see more intense rainfall in the lower basin, but the difference is merely 2.8%. For the entire basin (lower), the TOPMODEL shows "Good" modelling performance (0.75>NSE>0.65, 0.6>RSR>0.5), and the PDM shows satisfactory modelling performance (0.65>NSE>0.50, 0.7>RSR>0.6) (Moriasi et al., 2007). In terms of water balance, the bias is marked as "very good" ($P_{BIAS}<10$) for the TOPMODEL, and "good" ($10<P_{BIAS}<15$) for PDM. In the middle basin, "Good" performance is marked for the TOPMODEL, whereas PDM model classified as "Unsatisfactory" (NSE<0.5). It is important to note that the performance rating is based on monthly flow. Several authors agreed NSE value in the range of 0.15 to 0.3 is acceptable for daily flow simulation using SWAT model due to the difficulty and high variation at daily timestep (dos Santos et al., 2020). In the upper basin, "Unsatisfactory" is marked for both TOPMODEL and PDM. However, the water balance is close to the observation ($P_{BIAS}<10$). We attributed one possibility to the rainfall data recorded in the upper basin. Although the average annual rainfall is close (<2.8%) in the whole basin, the variation could be not well represented in the upper basin.

Figure 5 shows the modelling performance of daily flow in the lower basin yearly using TOPMODEL. The modelling performance is over 0.5 in 8 out of 11 years. The highest modelling performance is simulated in 2010 (NSE= 0.864), whereas

negative scores in 2019. Figure 6a shows that most of the flow regime are well simulated in 2010. In 2012, lower model performance is simulated. We found most of the peak events are still detected (Figure 6b), but the level of modelled peak flow is generally lower than the observed values. We must note that, rainfall data is replaced from nearby stations due to the high percentage of missing data in this year. The replaced rainfall data from could be less representative for the region. Lowest model performance is found in 2019 as we found the major gap of modelled and observed flow during March to June (Figure 6c). The representative of rainfall data could once again be the main issue. One example is the occurrence of intense rainfall in July, which has no influence found in the observed flow.

Uncertainty in rainfall data could be the main driver for the gap. Our research mainly uses rainfall data from 3 stations (expect in year 2012 and 2015, the data is replaced by using the time series from the nearest DAEE stations due to 40% of missing records) since continuous time-series data is hard to obtain in the study region. Despite the highly variation of rainfall data, the simulation shows that it is still representative of the most of modelling period. However, coarse data resolution could amplify under/overestimated rainfall in a single site (i.e. underestimated flow in 2012). In 2012, 2014, and 2019, the magnitude of flow is the main reason for the low modelling performance.

Despite certain gap exists, our results show that it is possible to use the JULES model for hydrological simulation in the Atibaia river basin. The model performance for daily flow is higher than the SWAT model's estimation (NSE=0.61 in the validation period) (dos Santos et al., 2020). However, both research pieces have pointed out that rainfall uncertainty is the primary reason for reduced model performance. There is a possibility for the model to be further improved once more adequate rainfall data is available.

4 Conclusions

We implemented the JULES6.1 model in the Atibaia river basin for hydrological estimation to evaluate the model performance. We evaluated the sensitivity of hydrological parameters to select the most suitable approach for the study region. We find that the TOPMODEL can reasonably estimate the flow. For PDM, improving modelling performance can be achieved after as these processes are sensitive to the hydrological parameters. Our results show that the JULES setup can detect most peak events and reasonably estimates baseflow. However, the uncertainty of rainfall data could be the primary driver for lower model performance in some period of higher rainfall variation. Nevertheless, our results suggest that it is possible to use the JULES model for hydrological evaluation in the Atibaia river basin. A more refined and higher quality of rainfall observation can be the fundamental drive to improve the modelling performance further.

Code and Data availability

This work was based on a version of JULES6.1. The instruction and configurations to run JULES is available from the JULES FCM repository

https://code.metoffice.gov.uk/trac/jules/wiki/WaysToRunJules

The configuration, code, and datasets for this research are available from

https://doi.org/10.5281/zenodo.5646468

Author contribution

185   HKC and MB led the writing and development of the manuscript. AMHdA processed the data and description of the study area. HKC developed the model and performed the simulations. All the authors contributed to the development of ideas and to the reflection process.

Acknowledgement

This work was funded by HEFCW GCRF Small Project: SP93 - Pilot flood and drought forecasting and early warning
190   system for Atibaia River Basin.

References

Best, M. J., Pryor, M., Clark, D. B., Rooney, G. G., Essery, R., Ménard, C. B., Edwards, J. M., Hendry, M. A., Porson, A., & Gedney, N. (2011). The Joint UK Land Environment Simulator (JULES), model description–Part 1: energy and water
195   fluxes. *Geoscientific Model Development, 4*(3), 677-699.

Brooks, R., & Corey, T. (1964). Hydraulic properties of porous media. *Hydrology Papers, Colorado State University, 24*, 37.

Buytaert, W., & Beven, K. (2011). Models as multiple working hypotheses: hydrological simulation of tropical alpine wetlands. *Hydrological Processes, 25*(11), 1784-1799.

Cavalcanti, I. F., Nunes, L. H., Marengo, J. A., Gomes, J. L., Silveira, V. P., & Castellano, M. S. (2017). Projections of
200   precipitation changes in two vulnerable regions of São Paulo State, Brazil. *American Journal of Climate Change, 6*(02), 268.

Clark, D. B., Mercado, L. M., Sitch, S., Jones, C. D., Gedney, N., Best, M. J., Pryor, M., Rooney, G. G., Essery, R., & Blyth, E. (2011). The Joint UK Land Environment Simulator (JULES), model description–Part 2: carbon fluxes and vegetation dynamics. *Geoscientific Model Development, 4*(3), 701-722.

205 Clark, D. B., & Gedney, N. (2008). Representing the effects of subgrid variability of soil moisture on runoff generation in a land surface model. *Journal of Geophysical Research: Atmospheres, 113*(D10)

Cox, P. M., Betts, R. A., Bunton, C. B., Essery, R., Rowntree, P. R., & Smith, J. (1999). The impact of new land surface physics on the GCM simulation of climate and climate sensitivity. *Climate Dynamics, 15*(3), 183-203.

de Campos, R. S., & Celso Dal Ré, C. (2015). Geologia da região de Atibaia e possíveis causas das inundações de 2009 e
210 2010.

Demanboro, A. C., Laurentis, G. L., & Bettine, S. d. C. (2013). Cenários ambientais na bacia do rio Atibaia. *Engenharia Sanitária E Ambiental, 18*(1), 27-37.

Dias, M. A. S., Dias, J., Carvalho, L. M., Freitas, E. D., & Dias, P. L. S. (2013). Changes in extreme daily rainfall for São Paulo, Brazil. *Climatic Change, 116*(3), 705-722.

215 dos Santos, F. M., de Oliveira, R. P., & Mauad, F. F. (2020). Evaluating a parsimonious watershed model versus SWAT to estimate streamflow, soil loss and river contamination in two case studies in Tietê river basin, São Paulo, Brazil. *Journal of Hydrology: Regional Studies, 29*, 100685.

FAO/IIASA/ISRIC/ISSCAS/JRC. (2012). Harmonized world soil database (version 1.2). *FAO, Rome, Italy and IIASA, Laxenburg, Austria,*

220 Friedl, M. A., & Sulla-Menashe, D. (2015). *MCD12Q1 MODIS/Terra+Aqua Land Cover Type Yearly L3 Global 500m SIN Grid V006*. NASA EOSDIS Land Processes DAAC. 10.5067/MODIS/MCD12Q1.006

Gedney, N., & Cox, P. M. (2003). The sensitivity of global climate model simulations to the representation of soil moisture heterogeneity. *Journal of Hydrometeorology, 4*(6), 1265-1275.

Harper, A. B., Wiltshire, A. J., Cox, P. M., Friedlingstein, P., Jones, C. D., Mercado, L. M., Sitch, S., Williams, K., & Duran-Rojas, C. (2018). Vegetation distribution and terrestrial carbon cycle in a carbon cycle configuration of JULES4. 6 with new plant functional types. *Geoscientific Model Development, 11*(7), 2857-2873.

Hodnett, M. G., & Tomasella, J. (2002). Marked differences between van Genuchten soil water-retention parameters for temperate and tropical soils: a new water-retention pedo-transfer functions developed for tropical soils. *Geoderma, 108*(3-4), 155-180.

Houldcroft, C. J., Grey, W. M., Barnsley, M., Taylor, C. M., Los, S. O., & North, P. R. (2009). New vegetation albedo parameters and global fields of soil background albedo derived from MODIS for use in a climate model. *Journal of Hydrometeorology, 10*(1), 183-198.

Jones, C., & Carvalho, L. M. (2013). Climate change in the South American monsoon system: present climate and CMIP5 projections. *Journal of Climate, 26*(17), 6660-6678.

Kanamitsu, M., Ebisuzaki, W., Woollen, J., Yang, S., Hnilo, J. J., Fiorino, M., & Potter, G. L. (2002). NCEP–DOE AMIP-II Reanalysis (R-2). *Bulletin of the American Meteorological Society, 83*(11), 1631-1643. 10.1175/BAMS-83-11-1631(2002)0832.3.CO;2

Le Vine, N., Butler, A., McIntyre, N., & Jackson, C. (2016). Diagnosing hydrological limitations of a land surface model: application of JULES to a deep-groundwater chalk basin. *Hydrology and Earth System Sciences, 20*(1), 143-159.

Maddox, R. A. (1983). Large-scale meteorological conditions associated with midlatitude, mesoscale convective complexes. *Monthly Weather Review, 111*(7), 1475-1493.

Marengo, J. A., Nobre, C. A., Seluchi, M. E., Cuartas, A., Alves, L. M., Mendiondo, E. M., Obregón, G., & Sampaio, G. (2015). A seca e a crise hídrica de 2014-2015 em São Paulo. *Revista USP,* (106), 31-44.

Marthews, T. R., Dadson, S. J., Lehner, B., Abele, S., & Gedney, N. (2015). High-resolution global topographic index values for use in large-scale hydrological modelling. *Hydrology and Earth System Sciences, 19*(1), 91-104.

Martínez-de la Torre, A., Blyth, E. M., & Weedon, G. P. (2019). Using observed river flow data to improve the hydrological functioning of the JULES land surface model (vn4. 3) used for regional coupled modelling in Great Britain (UKC2). *Geoscientific Model Development, 12*(2), 765-784.

Moore, R. J. (1985). The probability-distributed principle and runoff production at point and basin scales. *Hydrological Sciences Journal, 30*(2), 273-297.

Moriasi, D. N., Arnold, J. G., Van Liew, M. W., Bingner, R. L., Harmel, R. D., & Veith, T. L. (2007). Model evaluation guidelines for systematic quantification of accuracy in watershed simulations. *Transactions of the ASABE, 50*(3), 885-900.

Nobre, C. A., Marengo, J. A., Seluchi, M. E., Cuartas, L. A., & Alves, L. M. (2016). Some characteristics and impacts of the drought and water crisis in Southeastern Brazil during 2014 and 2015. *Journal of Water Resource and Protection, 8*(2), 252-262.

Ottoni, M. V., Ottoni Filho, T. B., Schaap, M. G., Lopes-Assad, M. L. R., & Rotunno Filho, O. C. (2018). Hydrophysical database for Brazilian soils (HYBRAS) and pedotransfer functions for water retention. *Vadose Zone Journal, 17*(1)

Prochmann, V. (2019). *Tecnologia desenvolvida pelo Simepar subsidia a gestão de bacias do Sistema Cantareira.* https://www.ufpr.br/portalufpr/noticias/tecnologia-desenvolvida-pelo-simepar-subsidia-a-gestao-de-bacias-do-sistema-cantareira/

Rossi, M. (2017). Mapa pedológico do Estado de São Paulo: revisado e ampliado. *São Paulo: Instituto Florestal, 1*, 118.

SABESP. (2020). *Portal dos Mananciais: Região Metropolitana de São Paulo.*

    http://mananciais.sabesp.com.br/HistoricoSistemas

265   Silveira, C. d. S., Souza Filho, Francisco de Assis de, Martins, Eduardo Sávio Passos Rodrigues, Oliveira, J. L., Costa, A. C.,

    Nobrega, M. T., Souza, S. A. d., & Silva, R. F. V. (2016). Mudanças climáticas na bacia do rio São Francisco: Uma

    análise para precipitação e temperatura. *Rbrh, 21*(2), 416-428.

Van Genuchten, M. T. (1980). A closed-form equation for predicting the hydraulic conductivity of unsaturated soils 1. *Soil*

    Science Society of America Journal, 44(5), 892-898.

270   Zulkafli, Z., Buytaert, W., Onof, C., Lavado, W., & Guyot, J. (2013). A critical assessment of the JULES land surface model

    hydrology for humid tropical environments. *Hydrology and Earth System Sciences, 17*(3), 1113-1132.
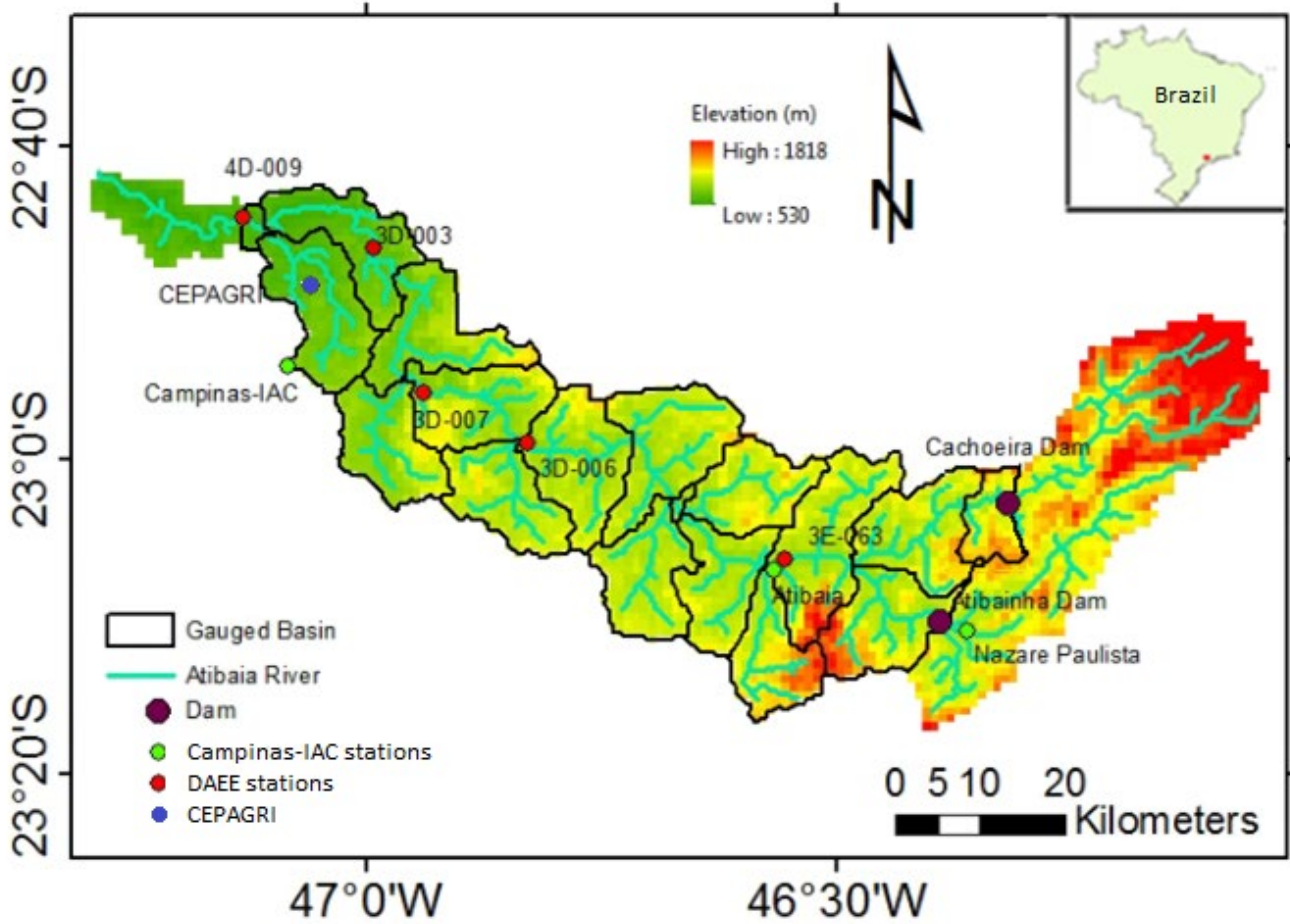
Figure 1: Atibaia river basin and the location of the rain gauges, flow monitoring stations, and dams.
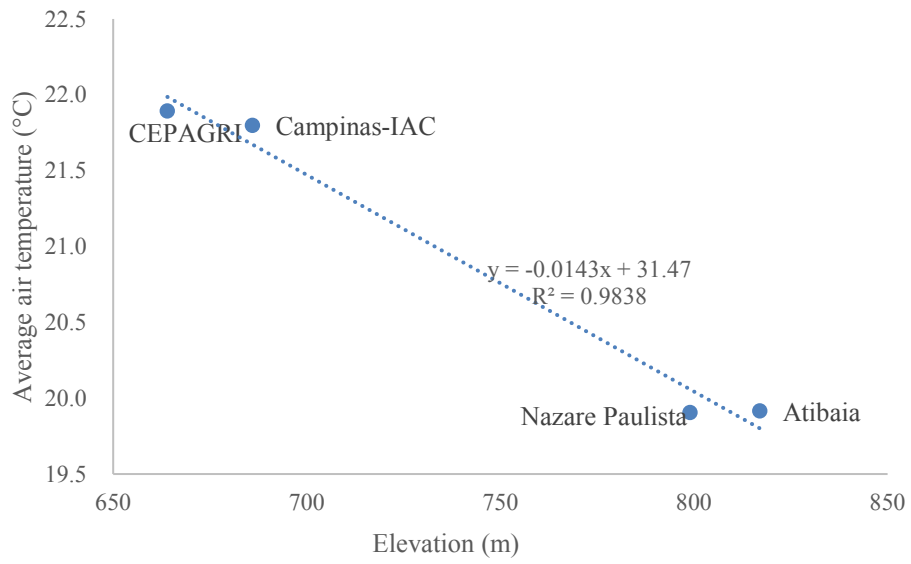
Figure 2. Average air temperature from 2009-2019 related to the site elevation.
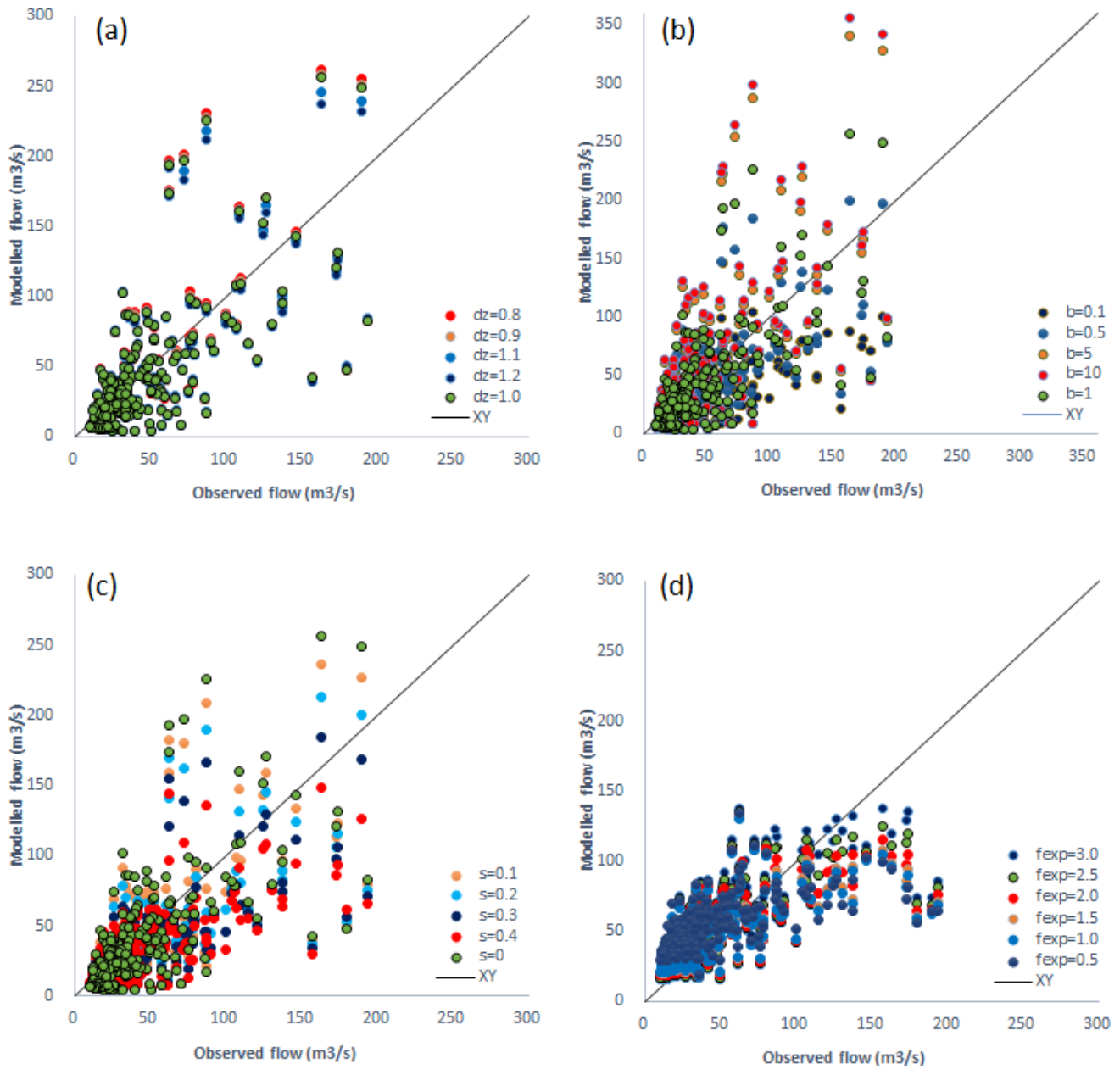
Figure 3. Sensitivity analysis of a) soil depth b) shape factor c) threshold of minimum soil water content, using PDM. d) Decay parameter, using TOPMODEL.
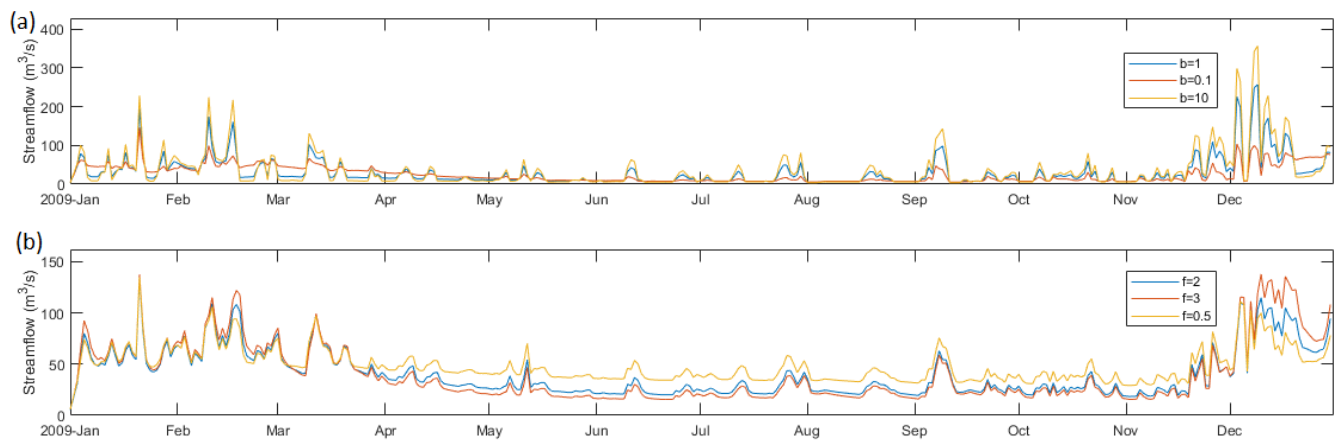
Figure 4. Daily modelled flow in the year 2009 using different (a) shape factors (PDM), (b) decay parameter (TOPMODEL).
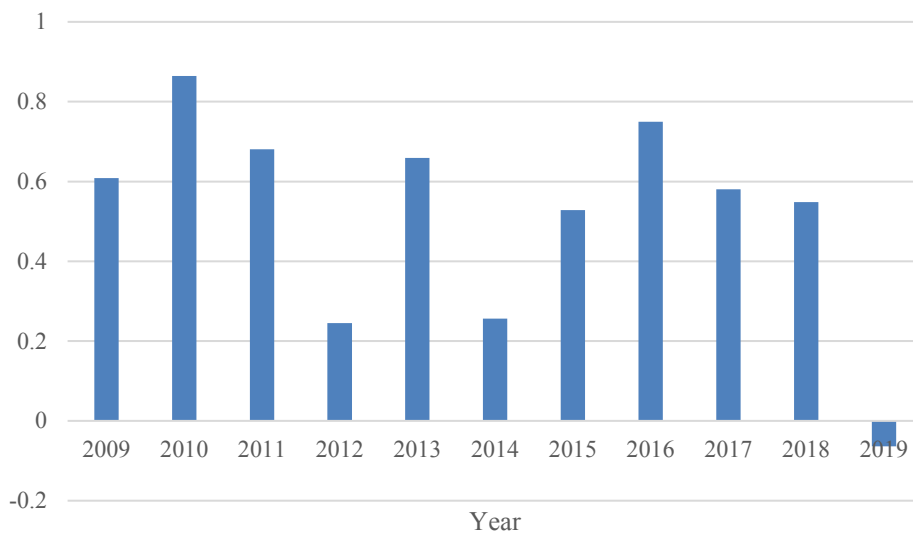
Figure 5. NSE score of modelling daily flow summarised by year (TOPMODEL).

285
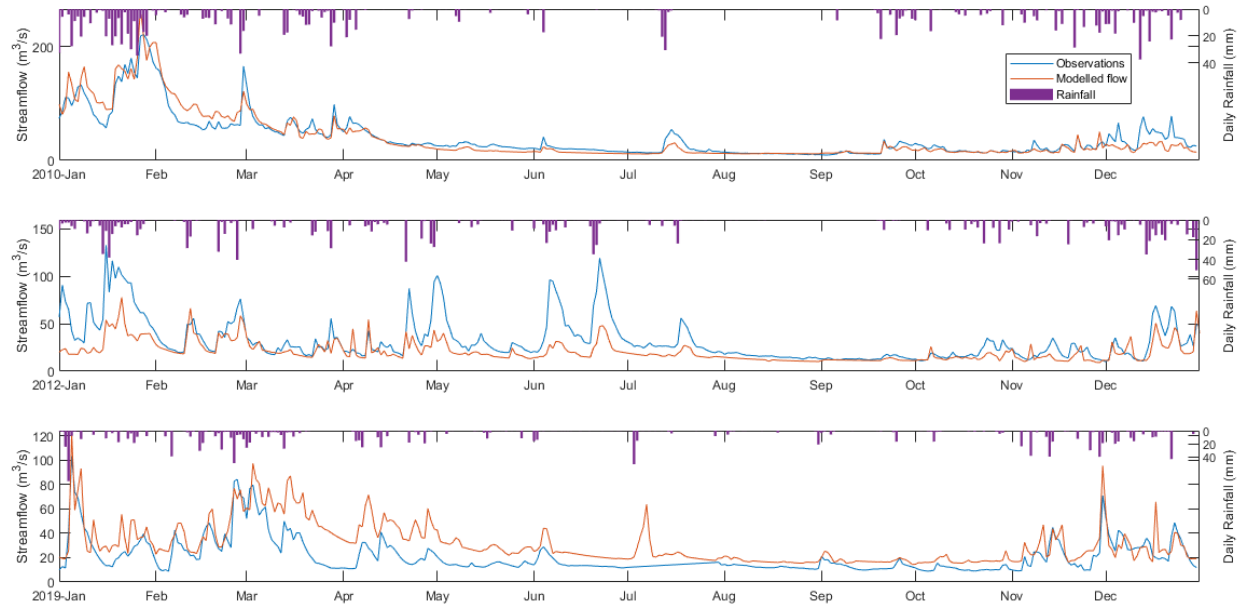
Figure 6. Daily modelled flow, observed flow, and rainfall in the year (a) 2010, (b) 2012 and (c) 2019 using TOPMODEL.

Table 1. Sensitivity analysis of hydrological parameters using 1) PDM and 2) TOPMODEL. Default parameter values underlined.

Parameter	Definition	Sensitivity analysis values
	PDM	
dz_pdm	The depth of soil considered by PDM (m)	0.8, 0.9, 1.0, 1.1, 1.2
b_pdm	Shape factor for the pdf	0.1, 0.5, 1, 5, 10
s_pdm	Minimum soil water content below which there is no surface runoff saturation excess production by PDM	0, 0.1, 0.2, 0.3
	TOPMODEL	
fexp	Decay parameter describing the decrease of the saturated hydraulic conductivity	0.5, 1, 1.5, 2, 2.5,3

Table 2. Modelling performance as calculated from the observed and modelled flow time series in lower, middle, and upper basin, using 1) TOPMODEL and 2) PDM. NSE: Nash Sutcliffe Efficiency. RMSE-observations standard deviation ratio. PBIAS: Percentage of bias

	Basin	Average annual rainfall [mm]	Average observed flow [m^3/s]	NSE	RSR	PBIAS
TOPMODEL	Lower	1314.0	26.9	0.69	0.56	-7.83
	Middle	1305.9	18.4	0.66	0.58	3.01
	Upper	1277.6	9.1	0.33	0.82	-5.41
PDM	Lower	1314.0	26.9	0.54	0.68	-12.21
	Middle	1305.9	18.4	0.45	0.74	-1.56
	Upper	1277.6	9.1	-0.30	1.14	-9.62